1-1-93
E7493

NASA Technical Memorandum 105970

An Integral Equation Solution for Multi-Stage Turbomachinery Design Calculations

Eric R. McFarland
Lewis Research Center
Cleveland, Ohio

Prepared for the
38th International Gas Turbine and Aero-engine Congress and Exposition
sponsored by the American Society of Mechanical Engineers
Cincinnati, Ohio, May 24–27, 1993

NASA

AN INTEGRAL EQUATION SOLUTION FOR MULTISTAGE TURBOMACHINERY DESIGN CALCULATIONS

Eric R. McFarland
National Aeronautics and Space Administration
Lewis Research Center
Cleveland, Ohio 44135

E-7493

ABSTRACT

A method has been developed to calculate flows in multistage turbomachinery. The method is an extension of quasi-three-dimensional blade-to-blade solution methods. Governing equations for steady compressible inviscid flow are linearized by introducing approximations. The linearized flow equations are solved using integral equation techniques. The flows through both stationary and rotating blade rows are determined in a single calculation. Multiple bodies can be modeled for each blade row, so that arbitrary blade counts can be analyzed. The method's benefits are its speed and versatility.

NOMENCLATURE

Bs,Bd,Bv	integral method influence coefficients
b	stream sheet thickness
C_p	pressure coefficient, $(P_t\text{-}P)/(\rho(r\Omega)^2/2)$
m	meridional coordinate
npt	number of panels
P	pressure
r	surface of revolution radius
S_1	blade-to-blade surface
s	surface distance
T	temperature
U	transformed wheel speed, $r^2\rho b\Omega$
V	absolute flow velocity
$V_{\rho b}$	estimated nonlinear term
v	absolute disturbance velocity
W	relative flow velocity
x,y	transformed coordinates
α	absolute flow angle with respect to meridional direction
γ,δ,σ	integral method sigularity strengths
θ	surface angle
ρ	fluid density
ϕ	tangential coordinate

Subscripts

c	uniform flow value
est	estimated value
i,j,k	panel index
m	meridional coordinate direction
n,t	normal, tangent to surface
onset	uniform flow value
p	point in flowfield
t	total/stagnation flow condition
x,y	transformed coordinate direction
ϕ	tangential coordinate direction

INTRODUCTION

Available tools for multistage turbomachinery design are limited. Axisymmetric throughflow calculations are the main design tool used for developing a multistage machine's flow path. These calculations predict the flow on a hub-to-shroud surface through the vane and blade rows. To estimate the flow on blade-to-blade surfaces, results from the throughflow calculation are used as input for another calculation. The additional calculation predicts the flow on a surface of revolution that is normal to the hub-to-shroud surface.

Many blade-to-blade solutions must be run for a multistage design. Solutions are run for several streamlines given by the hub-to-shroud calculations. Most blade-to-blade solutions are limited to calculating a single blade row's flowfield. Solutions are required for each blade row in the machine.

The combination of hub-to-shroud and blade-to-blade flow calculations has provided the basis of most designs in the past. More recently multiblade row Navier-Stokes calculations have become available to the turbomachinery designer. Rai (1987a), Jorgenson and Chima (1989), and Lewis et al. (1989) have displayed blade-to-blade stage calculations. Rai (1987b), Adamczyk et al. (1990), and Chen (1991) have reported on three-dimensional stage calculations.

These newer methods require significant computational resources. They typically have run times measured in hours on the fastest computers. These long run times limit the number of stages, the blade counts, and the variations in flow conditions that can be considered.

In some situations, the information yielded is well worth the time and effort spent in getting the solution. As progress on faster computers and better solution algorithms continues, the Navier-Stokes methods will become usable design tools. Now, they are used primarily to analyze designs that were arrived at using simpler means.

The need for a fast calculation of the blade-to-blade flowfield in multistage machines was the motivation for the work reported here. A question arose about a possible incidence problem in the Low Speed Axial Compressor (LSAC) facility being built at NASA Lewis Research Center. The compressor is four and one half stages. The blade row in question was the rotor row of the second stage.

The LSAC compressor is based on a similar facility at General Electric (Wisler, 1980). A throughflow design calculation existed for the compressor, but blade-to-blade analysis of the flowfield was not available. A simple potential flow solution was considered sufficient to answer the incidence question.

It was decided to calculate the blade-to-blade flowfield using the method of McFarland (1984). This method is a fast, robust blade-to-blade solution based on integral equation methods. Cascade flows have been analyzed with this method for many years.

The LSAC flowfield was calculated. The design has an inlet guide vane (IGV) followed by four identical stages. The solution method was applied to each blade row in turn, until the row of interest was reached. The calculated exit flow from one blade row became the upstream boundary condition of the next blade row in the flowpath. This is a common method of making an analysis of a multistage blade-to-blade flow.

This method of multistage flow analysis is flawed. The influence that one blade row has on the adjacent blade rows is neglected. Errors in the flowfield are introduced by considering each blade row as a separate flowfield. These errors are acceptable in a design calculation. Still, a solution that included all the blade rows in blade-to-blade flowfield would be better for finding the flow incidence.

During the calculation of the LSAC flow, I found that the integral equation method could be modified to calculate multistage flows in a single calculation. The modification was a simple change to the formulation of the method. The resulting method provides a fast means of calculating a multistage blade-to-blade flow.

At first, I thought that this formulation was new. In doing research for this paper, I later learned that it is not. Many of the basic ideas in the formulation had been previously described by Parker (1967). In this paper, I reformulate Parker's work, and incorporate it into an integral equation method. I also extend the method to subsonic compressible flows and radial flow machinery.

ANALYSIS

Governing Equations

The flow is assumed to be steady, inviscid, irrotational, and compressible. The governing equations for this flow are given in Eqs. (1) and (2). These equations are written for flow on a blade-to-blade surface of revolution. Equation (1) is the continuity equation, and Eq. (2) is the irrotationality condition. The equations are written with respect to an absolute frame of reference.

$$\frac{\partial}{\partial\phi}(\rho b V_\phi) + \frac{\partial}{\partial m}(r\rho b V_m) = 0 \tag{1}$$

$$\frac{\partial}{\partial\phi}(V_m) - \frac{\partial}{\partial m}(r V_\phi) = 0 \tag{2}$$

In Eqs. (1) and (2), V_m is the meridional velocity component, V_ϕ is the tangential velocity component, ρ is the fluid density, b is the stream sheet thickness, and r is the local radius of the axisymmetric blade-to-blade surface. The meridional direction is measured in the axial-radial plane along the surface of revolution. The tangential direction is measured in the circumferential direction. These equations should be recognizable as the equations of flow on the S_1 surface of Wu (1952).

McFarland (1984) showed that these equations can be transformed from flow on a surface of revolution to flow on a planer surface by using Eq. (3).

$$\begin{aligned} y &= \phi \\ x &= \int^m \frac{dm}{r} \\ V_x &= r\rho b V_m \\ V_y &= r\rho b V_\phi \end{aligned} \tag{3}$$

The transformation variables are written in terms of dimensionless coordinates. These coordinates appear similar to cartesian coordinates. They are denoted as x and y. Using these transformations, the governing equations become Eqs. (4) and (5).

$$\frac{\partial}{\partial y}\left(\frac{V_y}{r}\right) + \frac{1}{r}\frac{\partial}{\partial x}(V_x) = 0 \tag{4}$$

$$\frac{\partial}{\partial y}\left(\frac{V_x}{r\rho b}\right) - \frac{1}{r}\frac{\partial}{\partial x}\left(\frac{V_y}{\rho b}\right) = 0 \tag{5}$$

Equations (4) and (5) can be simplified by noting that r and b are functions of x. They can be further simplified by assuming that ρ is also a function of x only. This gives Eqs. (6) and (7).

$$\frac{\partial}{\partial y}V_y + \frac{\partial}{\partial x}V_x = 0 \tag{6}$$

$$\frac{\partial}{\partial y}V_x - \frac{\partial}{\partial x}V_y = -\frac{V_y}{\rho b}\frac{\partial}{\partial x}(\rho b) \tag{7}$$

Equation (7) is linearized by replacing the term on the right hand side of the equation by an estimated value. The estimated value can be calculated from results of a throughflow calculation or by making a one-dimensional flow calculation. The estimated term must be known before the solution of the flow equations is begun. The final form of Eq. (7) is given in Eq. (8).

$$\frac{\partial}{\partial y}V_x - \frac{\partial}{\partial x}V_y = -\frac{V_{y_{est}}}{(\rho b)_{est}}\frac{d}{dx}(\rho b)_{est} \tag{8}$$

Equations Solution

Equations (6) and (8) are linear. They can be solved by superposition of solutions. The solution is composed of a uniform flow plus a disturbance flow as shown in Eq. (9).

$$\begin{aligned} V_x &= V_{x_c} + v_x \\ V_y &= V_{y_c} + v_y \end{aligned} \tag{9}$$

Substituting Eq. (9) into the governing equations gives Eq. (10). The last equation in Eq. (10) is the estimated nonlinear term. It is a function x only.

$$\begin{aligned} V_{x_c} &= V_{onset}\cos(\alpha_c) \\ V_{y_c} &= V_{onset}\sin(\alpha_c) + V_{\rho b} \\ \frac{\partial}{\partial x}v_x &+ \frac{\partial}{\partial y}v_y = 0 \\ \frac{\partial}{\partial x}v_y &- \frac{\partial}{\partial y}v_x = 0 \\ V_{\rho b} &= \int^{(\rho b)_{est}}\left(\frac{V_y}{\rho b}\right)_{est} d(\rho b)_{est} \end{aligned} \tag{10}$$

These linear equations are amenable to solution by integral equations techniques. Integral equation solutions are often referred to as panel methods. In these methods, the flow equations are solved using distributed singularities such as source and vortex singularities. These singularities are located on the surface of the bodies.

The integral equation solution used in this study was developed by McFarland (1982) (1984). This solution was modified to calculate flows through multistage turbomachionery. In the original method, a frame of reference relative to the rotating bodies was used. The governing equations were written for relative flows. In the relative flow equations, the rotational speed of the bodies appeared as a additional term. The new method uses an absolute frame of reference. As can be seen in the above equations, the rotational speed of the bodies no longer explicitly appears in the governing equations. The rotation of blade rows is included in the solution through the surface boundary conditions.

Boundary Conditions

Three boundary conditions are used in determining a flowfield. The flow relative to a body is required to remain tangent to a body's surface. The flow is uniform upstream and downstream of the bodies. The circulation for each body is set by imposing a Kutta condition.

At any point on a body, the relative velocity is tangent to the body surface. This condition implies that the relative velocity normal to a surface is zero. It is expressed in Eq. (11). The relative velocity normal component, W_n, is known as a function of position on the body surface.

$$\overline{W}\cdot\overline{n} = W_n(s) = 0 \tag{11}$$

For the solution of this paper, the surface boundary condition needs to be given in terms of the absolute velocity, V. The absolute velocity is related to the relative velocity by the wheel speed, U. This relationship is given in Eq. (12).

$$\begin{aligned} \overline{V} &= \overline{W} + \overline{U} \\ U &= r^2\rho b\Omega \\ V_t &= W_t + U\sin(\theta) \\ V_n &= W_n + U\cos(\theta) \end{aligned} \tag{12}$$

In these equations, Ω is the rotational speed of a body, and θ is the angle of the surface with respect to meridional axis. For stationary bodies, Ω is zero. Equation (13) expresses the surface boundary condition for the absolute velocity.

$$V_n(s) = U(s)\cos\left[\theta(s)\right] \tag{13}$$

The final form of the surface boundary condition is given by Eq. (14). This equation is written in the form use in the

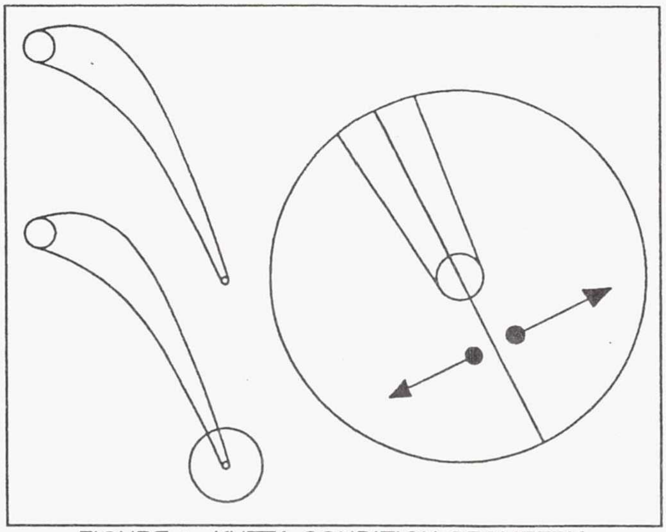

FIGURE 1. KUTTA CONDITION GEOMETRY.

integral equation solution of McFarland (1982). The terms without summations are the uniform flow part of the solution. The summation terms are the disturbance flow part of the solution. In the summations, Bs, Bv, and Bd parameters are the influence coefficients used in the integral equations. The σ, γ, and δ variables are the source, vortex, and vortex jump singularity distrbutions calculated in the integral equation solution.

$$0 = -V_{onset} \sin(\theta_p - \alpha_c) + (V_{\rho b_p} - U_p) \cos(\theta_p) + \sum_{i=1}^{npt-1} Bs_{pi}\sigma_i + \sum_{j=1}^{npt} Bv_{pj}\gamma_j + \sum_{k=1}^{m} Bd_{pk}\delta_k \tag{14}$$

As can be seen in Eq. (14), the surface boundary condition is included as part of the uniform flow solution. Each body in the problem can have a rotational velocity assigned to it. This makes the calculation of flows for machines that have blade rows rotating at different speeds or in opposite directions easy to accommodate.

The uniform flow conditions for the upstream and downstream boundaries are combined with the Kutta condition to set the overall circulation of the flowfield. These conditions are similar to those used by McFarland (1984). For the present solution, the upstream and downstream boundary conditions and circulation calculation are reformulated in terms of the absolute velocity.

Kutta Condition

A Kutta condition is used to set the circulation for each body. The use of a Kutta condition is a key feature of this solution. Its formulation significantly effects the flowfield solution.

The Kutta condition of McFarland (1982) is used. The description of this Kutta condition is repeated here. Two points are located just downstream of the trailing edge of each body. The points lie an equal distance from the trailing edge bisector as shown in Fig. 1. A coordinate system is assigned to each point. This coordinate system is usually aligned with the direction of the trailing edge bisector of the body. A different alignment direction can be specified. This gives a means for modeling deviation and slip flows. The relative velocities normal to the assigned direction at each point are required to be of equal magnitudes but of opposite signs. This forces the relative flow to leave the body's trailing edge smoothly. The Kutta condition in this solution was reformulated using absolute velocity and wheel speed.

Solution

The solution equations are similar to those given by McFarland (1982). The source strength is assigned a value equal to the normal component of the uniform flow along a body's surface. A normal velocity boundary condition (Eq. (14)) is written for each panel that is used to model the body shape. A tangential error minimization equation is written for each surface discontinuity on a body. The Kutta condition is applied to the trailing edge flow of each body. This system of equations is solved by using upper and lower triangular matrix decomposition.

Solution of the above system of equations gives a flowfield that satisfies the surface boundary conditions and the Kutta condition. To simultaneously satisfy the upstream and downstream boundary conditions, an iterative process is used. The iteration variable is α_c, the flow angle of the uniform flow. This angle is adjusted until the calculated upstream flow angle matches the specified upstream flow angle.

Flow Estimate

The final piece of the solution is the calculation of the flow estimate. The flow estimate is used to replace the nonlinear term in Eq. (7). This term is zero for incompressible flows with constant stream sheet thickness. For compressible flows, it has a significant effect on solution results. The quality of the flow parameters used in calculating the term has a direct impact on the solution. A poor estimate will result in a poor compressible flow solution.

The flow estimate is also used to include energy effects into the solution. Energy effects are not usually considered in single blade row calculations. For these calculations, the blade row is either rotating or stationary. The energy equation can be replaced by specifying constant rothalpy or enthalpy.

Since both rotating and stationary blades are present in this solution, the total energy of the system is not constant. The energy will increase as a rotor compresses the flow. Work is

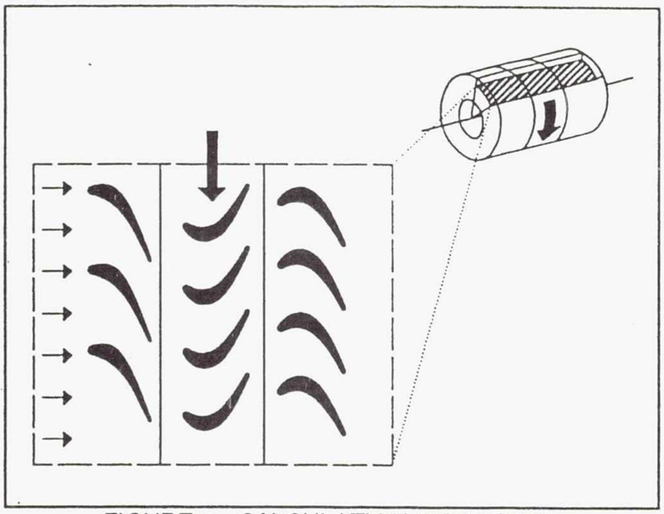

FIGURE 2. CALCULATION GEOMETRY.

done on the system, and the absolute total temperature of the flow increases. If the flow is expanded through the rotor, the reverse occurs. The absolute total temperature of the flow decreases.

A flow estimate can be provided in two ways. In the first way, the results from a throughflow calculation can be used directly as the estimate. The second way is to make a one-dimensional calculation of the blade-to-blade flow. The estimated values are calculated from the one-dimensional results.

The one-dimensional flow calculation was used in this paper. The flowpath was divided into segments of rotating and stationary blade rows. Each flowpath segment was subdivided into a number of steps. The given flowpath and blade geometries were used to calculate the flow area along the flowpath. The relative flow was assumed to follow the average turning of the blade shapes inside the blade rows. Outside the blade rows, interpolation was used to get the flow conditions. At each flowpath step, the one-dimensional flow equation, constant rothalpy condition, calculated flow area, and assumed flow turning were used to calculate the density and relative velocity. The calculated relative velocity was combined with the geometry information to give the absolute velocity and wheel speed. These velocities are used in a simple energy equation to give the absolute total temperature variation along the flowpath. Finally, the results are numerically integrated along the flowpath to give the estimated nonlinear term, V_{pb}.

RESULTS AND DISCUSSION

The method was verified by comparing solution results with experimental data from United Technology Research Center's (UTRC) Large Scale Rotating Rig facility. Experimental results from this research facility have been presented in numerous papers. Five of these papers were used in making the comparisons presented here. These papers are Dring, Joslyn, and Blair (1987); Dring et al. (1986); Joslyn, Dring, and Sharma (1983); and Dring et al. (1982) (1981).

The UTRC large scale turbine test geometry was analyzed. The experiment is described in detail by Dring (1986). The test configuration was a one and one half stage axial turbine. Blade counts for first stator row, rotor row, and second stator row were 22, 28, and 28 respectively. The mean radius of the stage was 0.686 m. (27 in.). Hub and shroud walls were cylindrical. The axial spacing between the blade rows was variable. The turbine vane and blade shapes were typical of 1980 designs. The inlet velocity was 23 m/s (75 f/s). The rotational speed was 410 rpm. This rotational speed gave an axial velocity to mean wheel speed ratio of 0.78. This was the design ratio for the turbine.

The UTRC turbine experiment provides a simple test case. The main feature of the flowfield is the interaction of the blade rows. The experiment had low Mach number flows. Compressible flow effects were small. The flowpath geometry was axial and large scale. Radius and stream sheet thickness changes were negligible. The midspan flow was nearly two-dimensional.

The experiment's simple flowfield made it a good choice for use in verifying the method presented here. The method's new capability to calculate interacting blade row flows could be explored independently from other factors that effect the flow.

Steady Flow Results

The first test case analyzed had the rotor row located midway between the two stator rows. This case was selected since the unsteady and viscous wake effects of the flow are minimized. The large spacing between the two stator rows and the rotor row allows the flow to circumferentially mix between rows. The configuration is designated as the 50 percent case by Dring (1987).

The midspan blade-to-blade geometry used to model the experiment is shown in Fig. 2. The calculation uses periodic circumferential sectors. The arc of a sector is 2π divided by the number of sectors. The number of sectors is chosen to match a row's blade count. The number of sectors times the number of blades contained in the sector for each row should equal the blade count for that row. If all blade rows have the same blade count, the sector pitch will be equal to the blade row pitch. This is rarely the case in turbomachinery design because of aeroelastic problems that result from equal blade counts. A sector of blades is usually selected for the calculation that contains an integer ratio of blades in the rows. The worst case is for one row's blade count to be a prime number. In this case the sector pitch will be 2π, and it will contain all the blades in the rows.

The calculation's blade count did not match the experimental configuration. The blade count was altered to reduce the computational resources required to make the calculation. The case was modeled as seven periodic sectors of three stator vanes followed by four rotor blades followed by four stator vanes. This causes the first stator row's blade count to be 21

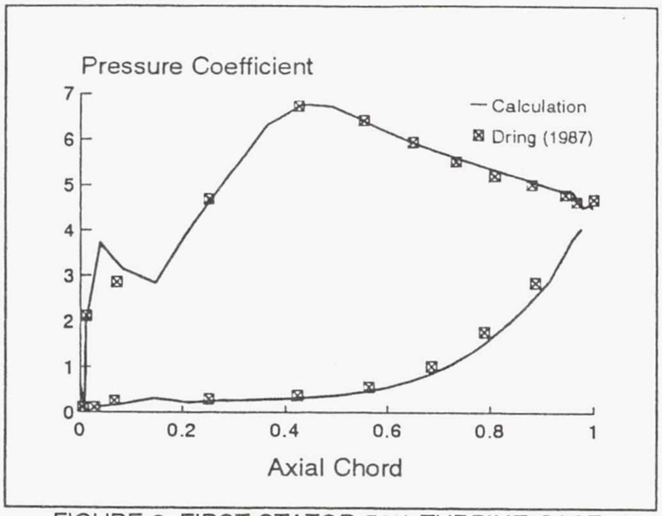

FIGURE 3. FIRST STATOR 50% TURBINE CASE.

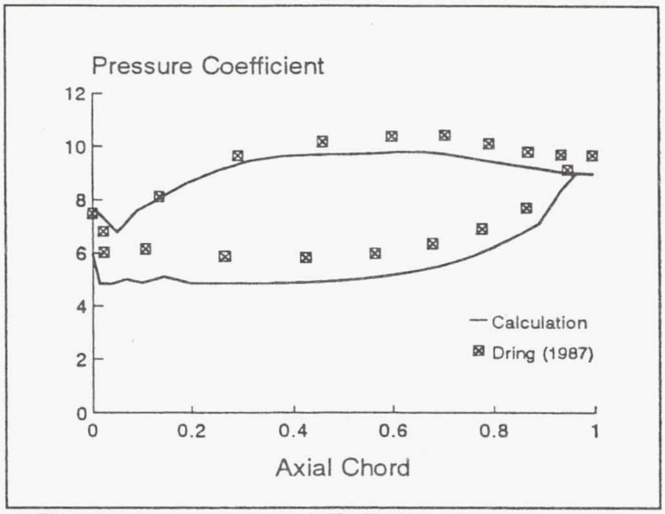

FIGURE 5. SECOND STATOR 50% TURBINE CASE.

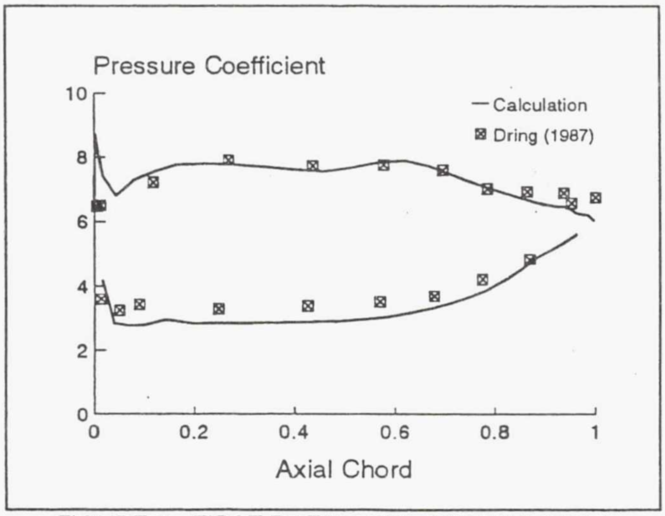

FIGURE 4. FIRST ROTOR 50% TURBINE CASE.

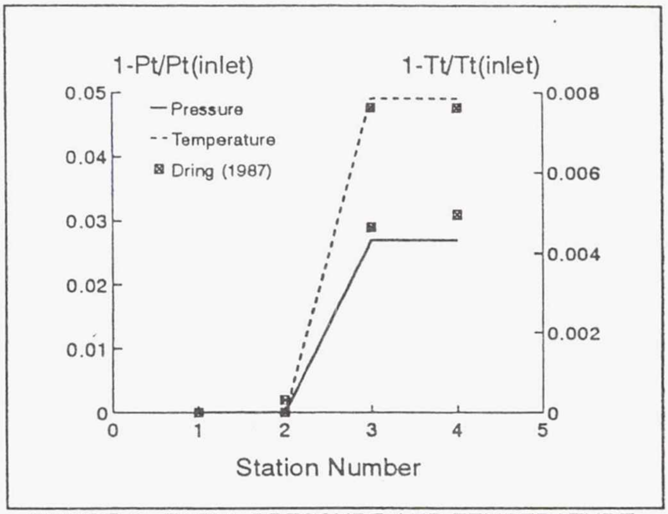

FIGURE 6. TOTAL PRESSURE AND TEMPERATURE.

instead of 22. It's pitch is about 5 percent greater than the experiment. No scaling of the stator geometry was made to compensate for the increased pitch.

Results of the calculation are shown in Figs. 3 to 5. The figures show pressure coefficient as a function of the normalized axial chord. The pressure coefficient (Eq. 15) has the same form as used by Dring (1987).

$$C_p = \frac{P_t(\text{inlet}) - P}{\frac{1}{2}\rho(r\Omega)^2} \tag{15}$$

The calculated surface pressures are compared with the experiment. The calculated pressures are the average of the pressures for each blade in a row of the sector. The calculated pressures varied very little between blades in a row. The experimental values are the time average pressures measured on a single blade in a row.

Overall, the comparison is good. The comparison is very good for the first stator row. However as the surface pressures are calculated further along the flowpath, the comparison becomes poorer. The tangential loading appears correct for all three rows, but the absolute level is off for the rotor and second stator.

The reason for the increasing error along the flowpath is a loss in total pressure. The calculation assumes that the total pressure varies only with total temperature. As seen in Fig. 6, the calculation models the total temperature drop through the rotor accurately. The temperature change is related to the

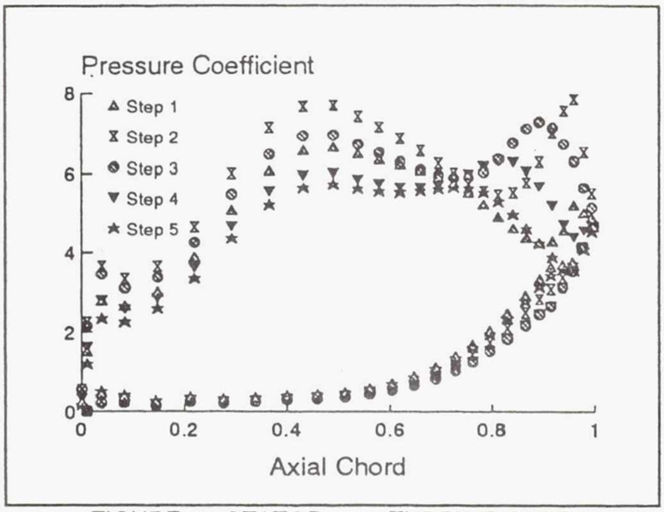

FIGURE 7. STATOR 15% TURBINE CASE.

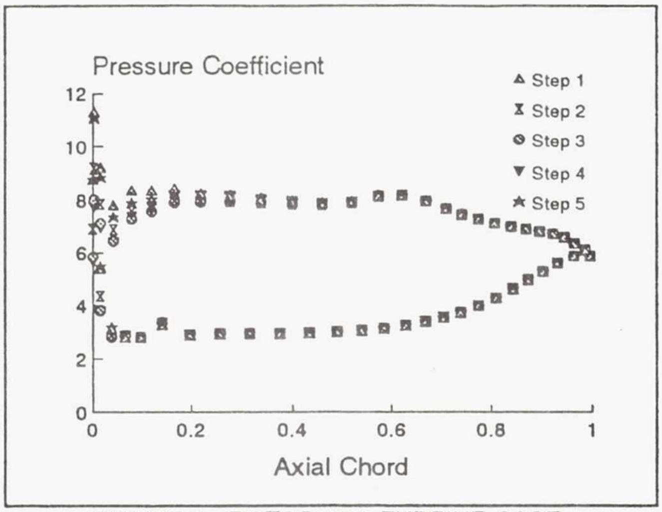

FIGURE 8. ROTOR 15% TURBINE CASE.

turning of the flow by the rotor. Figure 4 showed that the calculated and measured rotor loading were very close. Where the calculation falls down is in the total pressure calculation. The loss in total pressure due to viscous flow and mixing has not been included. This can be seen in Fig. 6 as the increasing difference in calculated and measured total pressure.

For the solution to be viable, a loss model needs to be added. Techniques are available to correct inviscid solutions for total pressure loss. A user specified adiabatic efficiency for each blade row will be added to this method. The calculated total temperature change is assumed to be correct. The specified efficiency will be used to correct the total pressure for losses. Including this loss model into the method, should be straightforward.

Dynamic Loading Results

The method has features that make it appear like an unsteady solution. Both rotating and stationary blade rows are present. Blade loading can vary from blade to blade in a row. It is tempting to try to infer unsteady flow information from the solution. However the solution is steady state. Time derivatives are not included in the governing equations. The most that could be determined from the solution is the amplitude of the pressure variations along a blades surface.

The closely coupled case from the UTRC turbine experiment was analyzed to explore the ability of the method to predict periodic loading variations. Dring (1987,1982,1981) referred to this configuration as the 15 percent case. The test consisted of a single turbine stage. The rotor row was placed 15 percent of the axial chord downstream of the stator row. The inlet flow and rotational speed were the same as were used in the steady state results. The calculation used two periodic sectors of 11 vanes and 14 blades. This matches the blade count of the experiment exactly. The blade-to-blade surface was taken at midspan.

Calculated variations in the stator and rotor surface pressure with rotor position are shown in Figs. 7 and 8. The pressure distribution are for an individual vane and blade. The five distributions shown on the figures are from five separate calculations. The variation in the distribution is the result of moving the rotor blades one fifth the rotor row's pitch in the tangential direction for each calculation. The series of solutions represents the periodic pressure variations the blades should experience in the experiment.

The general shape of the loading variations matches Dring's description (1982). The large variations in pressure at the vane trailing edge and rotor leading edge are present in the solution. The narrowing of the variations at the vane throat on the suction, and smaller pressure fluctuations on the pressure surface are also predicted.

The solution does not model the pressure changes inside the rotor passage that are due to the vane wakes. As these wakes move downstream, they are distorted by the rotor flow. This produces the pressure fluctuations measured in the experiment. The calculation does not account for these wakes, so these fluctuations are not present in the solution.

Further comparisons with Dring's experimental data (1981), shows that the calculation does not model the amplitude of the unsteady pressure variation very well. Figures 9 and 10 show the comparisons. In these figures the blade leading edge is located at zero on the axial chord axis. The negative axial chord axis is the pressure surface of the blade. The positive axial chord axis is the suction surface. The differential pressure coefficient is calculated as the difference between the maximum and minimum pressure that the blade surface experiences during the periodic passing of the rotor.

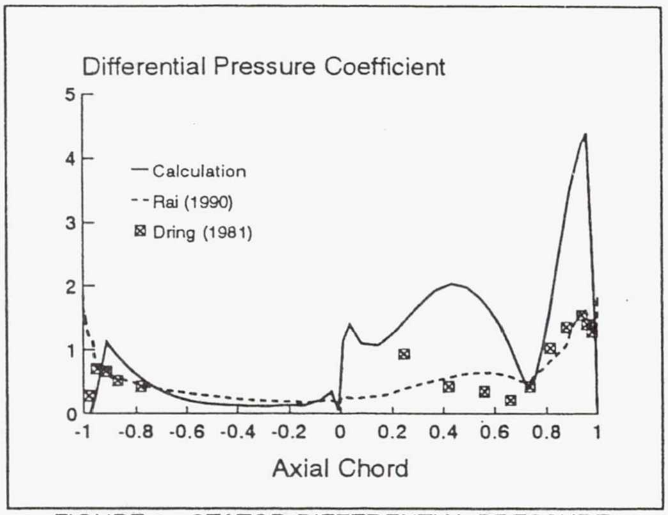

FIGURE 9. STATOR DIFFERENTIAL PRESSURE.

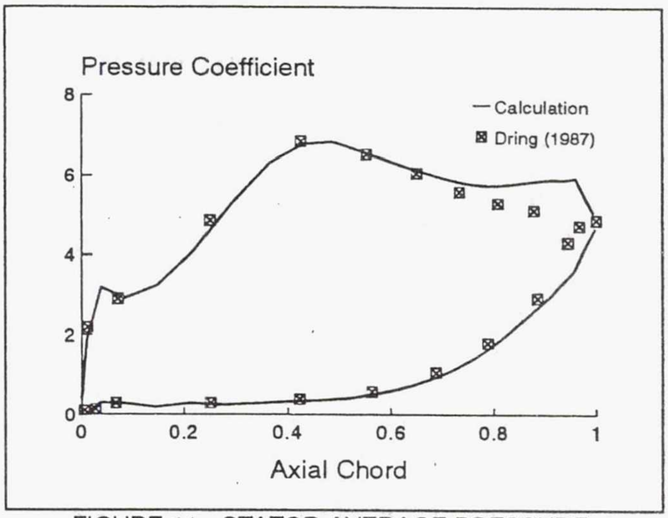

FIGURE 11. STATOR AVERAGE PRESSURE.

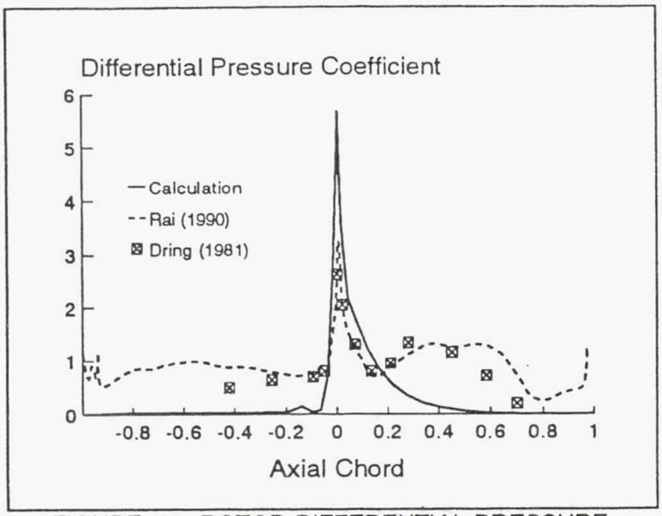

FIGURE 10. ROTOR DIFFERENTIAL PRESSURE.

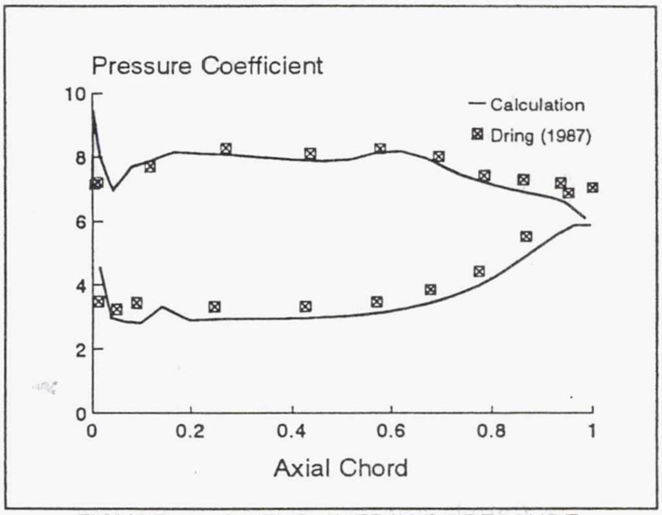

FIGURE 12. ROTOR AVERAGE PRESSURE.

The calculation does match the data at a few points, but in general it poorly predicts the magnitude of the unsteady pressure. Over most of the vane surface and the rotor leading edge the pressure difference is over predicted. Inside the rotor passage, the pressure is under predicted. Figure 10 clearly shows the pressure fluctuations inside the rotor passage are not modeled by the solution.

From these results, it is apparent that one of the effects of the unsteady flow terms on the potential interaction of rotor/stator flows is to attenuate the magnitude of pressure variations. This is consistent with the findings of Kemp and Sears (1953).

The solution of Rai and Madavan (1990) is included on Figs. 9 and 10 for comparison. This is an unsteady Navier-Stokes analysis of Dring's experiment. This calculation has a more complex model of the flow physics. As expected, it gives a better prediction of the unsteady flow pressures.

The last comparisons with the 15 percent case are shown in Figs. 11 and 12. The calculated results in the figures show the arithmetic average of the pressure distributions shown in Figs. 7 and 8. The experimental data is the time averaged surface pressures. The comparison is good.

The calculation could be made to agree better with the experiment. The arithmetic average of the calculation results could be time weighted to more accurately model the time averaging of the experiment. Smaller steps could be used in moving the rotor. The resulting arithmetic average would more closely approximate a time average. Instead of averaging the surface pressure from a single vane and blade, all 11 vanes and

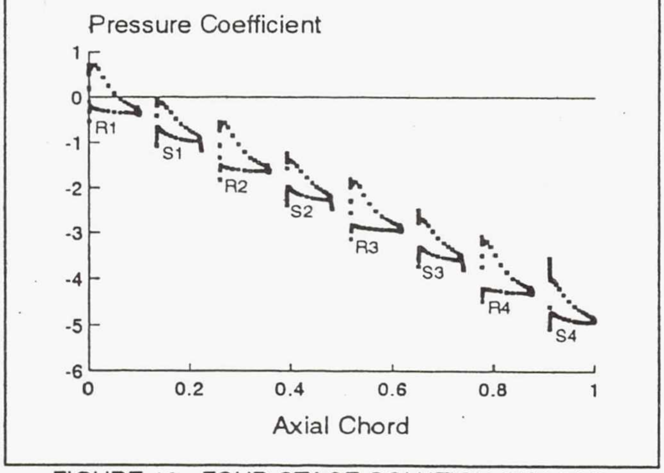

FIGURE 13. FOUR STAGE SOLUTION OF LSAC.

14 blades pressure distributions in the solution could be used. The larger sample of pressure distributions would give a better prediction of the time average pressure.

Example Solution

To demonstrate the solution method, results from the analysis of the LSAC design will be given. The analysis is for a blade-to-blade surface near the compressor's hub. The LSAC consists of a set of IGVs followed by four identical stages. It was modeled as 13 periodic sectors of 4 IGVs followed by 4 stages of 3 rotors and 4 stators each. This matches the blade count of the LSAC. The inlet flow velocity was 19.6 m/s (64.2 ft/s), the rotational speed was 960 rpm, and the radius was 0.488 m (1.6 ft). These conditions are consistent with design flow along the hub of the LSAC.

Results from the calculation are shown in Fig. 13. Only the pressure loadings for the four stages are shown. The first pressure distribution is for the first rotor. It is followed by the loading for the first stator. The loading distributions continue with a rotor followed by stator for the next three stages.

No experimental data was available for comparison. The loading is similar for all rotors and all stators. The static pressure rise is linear with axial distance. Both these results are expected since the stages are identical.

Computational Times

In design, it is desirable for a solution method to run quickly. With a faster method, a designer can look at more cases. This expands the design space that a designer can explore in a given amount of time.

The multistage integral method is very fast compared to other multistage methods. The use of linear flow equations for the solutions contributes the most to the method's speed. The use of an integral equation solution also makes the method faster, because the dimensionality of the problem is reduced by one. The integral equations are written for line integrals around the bodies. A flowfield grid is not required. This reduces the size of the computation, and allows the user to skip the usual step of generating a flowfield grid.

The flow cases presented were run on the Cray YMP at NASA Lewis Research Center. The 50 percent turbine case had seven bodies with 50 panels each. The CPU time was 223 sec. The 15 percent turbine case had 25 bodies with 50 panels each. Its CPU time was 327 sec/step. The four and one half stage LSAC case had 32 bodies with 60 panels each. This case required 913 sec to run.

Although all the cases presented were run on a Cray YMP, smaller problems have been run on less powerful computer systems. A single stator followed by a rotor followed by a stator model of the UTRC turbine experiment was run on a personal computer with a 20 Mz clock speed. The solution convereged in 266 sec. The same case running on the YMP computer required less than 10 sec.

CONCLUSION

A method has been developed for analyzing multistage turbomachinery flows. The method solves a linear set of equations. It provides a rapid means of calculating blade-to-blade flows in multistage machines. It should be a useful design tool.

The method was shown to predict low speed axial turbine flows well. The comparison of solution results with time averaged experimental data was good. As one would expect, the lack of a loss model was found to be a shortcoming of the method.

An attempt was made to predict the periodic variations in surface pressures experienced in closely coupled multistage machines. The results of the attempt showed that the method only crudely modeled these flows. The lack of unsteady and vicous flow terms in the governing equations cause the method to inaccurately calculate the variations in unsteady blade loading.

Preliminary results from the method have been presented. These results are encouraging. Further study and development of the method are warranted. The ability of the method to predict higher Mach number flows and multistage radial turbomachinery should be explored. A total pressure loss model needs to be incorporated in the calculation. More cases need to be analyzed with the method to verify its capabilities, and better define its usefulness in turbomachinery design.

ACKNOWLEDGMENT

The author would like to thank Dr. Daniel Hoyniak and Dr. John Adamczyk of NASA Lewis Research Center for their comments on the relationship of this method to unsteady flows.

REFERENCES

Adamczyk, J.J., Celestina, M.L., Beach, T.A., and Barnett, M., 1990, "Simulation of Three-Dimensional Viscous Flow Within a Multistage Turbine," Journal of Turbomachinery, Vol. 112, pp. 370–376.

Chen, J.P., 1991, "Unsteady Three-Dimensional Thin-Layer Navier-Stokes Solutions for Turbomachinery in Transonic Flow," Ph.D. Thesis, Mississippi State University, MS.

Dring, R.P., Joslyn, H.D., Hardin, L.W., and Wagner, J.H., 1981, "Research on Turbine Rotor-Stator Aerodynamic Interaction and Negative Incidence Stall," Report AFWAL–TR–81–2114.

Dring, R.P., Joslyn, H.D., Hardin, L.W., and Wagner, J.H., 1982, "Turbine Rotor-Stator Interaction," Journal of Engineering for Power, Vol. 104, pp 729–740.

Dring, R.P., Blair, M.P., Joslyn, H.D., Power, G.D., and Verdon J.M., 1986, "The Effects of Inlet Turbulence and Rotor/Stator Interactions on the Aerodynamics and Heat Transfer of a Large-Scale Rotating Turbine Model, I—Final Report," NASA CR–4079.

Dring, R.P., Joslyn, H.D., and Blair, M.P., 1987, "The Effects of Inlet Turbulence and Rotor/Stator Interactions on the Aerodynamics and Heat Transfer of a Large-Scale Rotating Turbine Model, IV—Aerodynamic Data Tabulation," NASA CR–179469.

Jorgenson, P.C.E., and Chima R.V., 1989, "An Unconditionally Stable Runge-Kutta Method for Unsteady Flows," AIAA Paper 89–0205.

Joslyn, H.D., Dring, R.P., and Sharma, O.P., 1983, "Unsteady Three-Dimensional Turbine Aerodynamics," Journal of Engineering for Power, Vol. 105, pp 322–331.

Kemp, N.H., and Sears, W.R., 1953, "Aerodynamic Interference Between Moving Blade Rows," Journal of the Aeronautical Sciences, Vol. 20, No. 9, pp 585–597.

Lewis, J.P., Delaney, R.A., and Hall, E.J., 1989, "Numerical Prediction of Vane-Blade Aerodynamic Interaction," Journal of Turbomachinery, Vol. 111, pp 387–393.

McFarland, E.R., 1982, "Solution of Plane Cascade Flow Using Improved Surface Singularity Methods," Journal of Engineering for Power, Vol. 104, pp 668–674.

McFarland, E.R., 1984, "A Rapid Blade-to-Blade Solution for Use in Turbomachinery Design," Journal of Engineering for Power, Vol. 106, pp 376–382.

Parker, R., 1967, "Calculation of Flow Through Cascades of Blades Having Relative Motion and The Generation of Alternating Pressures and Forces Due to Interaction Effects," Proceedings of the Institute of Mechanical Engineering, Vol. 182, Pt. 1, No. 11, pp 229–242.

Rai, M.M., 1987a, "Navier-Stokes Simulations of Rotor-Stator Interaction Using Patched and Overlaid Grids," Journal of Propulsion and Power, Vol. 3, No. 5, pp 387–396.

Rai, M.M., 1987b, "Unsteady Three-Dimensional Navier-Stokes Simulation of Turbine Rotor Interaction," AIAA Paper 87–2058.

Rai, M.M., and Madavan, N.K., 1990, "Multi-Airfoil Navier-Stokes Simulations of Turbine Rotor-Stator Interaction," Journal of Turbomachinery, Vol. 112, pp 377–384.

Wisler, D.C., 1980, "Core Compressor Exit Stage Study, Volume II—Data and Performance Report for the Baseline," NASA CR–159498.

Wu, C.-H., 1952, "A General Theory of Three-Dimensional Flow in Subsonic and Supersonic Turbomachines of Axial-, Radial-, and Mixed-Flow Types," NACA TN–2604.

REPORT DOCUMENTATION PAGE

Form Approved
OMB No. 0704-0188

1. AGENCY USE ONLY (*Leave blank*)	2. REPORT DATE	3. REPORT TYPE AND DATES COVERED
	May 1993	Technical Memorandum

4. TITLE AND SUBTITLE

An Integral Equation Solution for Multi-Stage Turbomachinery Design Calculations

5. FUNDING NUMBERS

WU–505–62–52

6. AUTHOR(S)

Eric R. McFarland

7. PERFORMING ORGANIZATION NAME(S) AND ADDRESS(ES)

National Aeronautics and Space Administration
Lewis Research Center
Cleveland, Ohio 44135–3191

8. PERFORMING ORGANIZATION REPORT NUMBER

E–7493

9. SPONSORING/MONITORING AGENCY NAMES(S) AND ADDRESS(ES)

National Aeronautics and Space Administration
Washington, D.C. 20546–0001

10. SPONSORING/MONITORING AGENCY REPORT NUMBER

NASA TM–105970

11. SUPPLEMENTARY NOTES

Prepared for the 38th International Gas Turbine and Aero-engine Congress and Exposition sponsored by the American Society of Mechanical Engineers, Cincinnati, Ohio, May 24–27, 1993. Responsible person, Eric R. McFarland, NASA Lewis Research Center, (216) 433–5915.

12a. DISTRIBUTION/AVAILABILITY STATEMENT

Unclassified - Unlimited
Subject Category 07

12b. DISTRIBUTION CODE

13. ABSTRACT (*Maximum 200 words*)

A method has been developed to calculate flows in multistage turbomachinery. The method is an extension of quasi-three-dimensional blade-to-blade solution methods. Governing equations for steady compressible inviscid flow are linearized by introducing approximations. The linearized flow equations are solved using integral equation techniques. The flows through both stationary and rotating blade rows are determined in a single calculation. Multiple bodies can be modelled for each blade row, so that arbitrary blade counts can be analyzed. The method's benefits are its speed and versatility.

14. SUBJECT TERMS

Multi-stage; Turbomachinery; Blade-to-blade

15. NUMBER OF PAGES

12

16. PRICE CODE

A03

17. SECURITY CLASSIFICATION OF REPORT	18. SECURITY CLASSIFICATION OF THIS PAGE	19. SECURITY CLASSIFICATION OF ABSTRACT	20. LIMITATION OF ABSTRACT
Unclassified	Unclassified	Unclassified	

National Aeronautics and
Space Administration

Lewis Research Center
Cleveland, Ohio 44135

NASA